



# EUROPEAN SOUTHERN OBSERVATORY

Organisation Européenne pour des Recherches Astronomiques dans l'Hémisphère Austral  
Europäische Organisation für astronomische Forschung in der südlichen Hemisphäre

ESO - European Southern Observatory  
Karl-Schwarzschild Str. 2, D-85748 Garching bei München

---

## Very Large Telescope Paranal Science Operations MIDI User Manual

Doc. No. VLT-MAN-ESO-15820-3519

Issue 89, Date 22/11/2011

Prepared ..... Th. Rivinius  
Date Signature

Approved ..... A. Kaufer  
Date Signature

Released ..... C. Dumas  
Date Signature

This page was intentionally left blank

### Change Record

Issue	Date	Section/Parag. affected	Reason/Initiation/Documents/Remarks
89	22 Nov, 2011	—	Version for P89
88	24 Feb, 2011	4.4.2,6.1	Version for P88, correlated flux mode for UTs
87	23 Aug, 2010	—	Version for P87, FINITO mode decomm., 25 min. per OB
86	27 Feb, 2010	—	Version for P86
85	20 Aug, 2009	4.4, 5.3	Field mode decomm., FINITO w/ AT only
84	31 Jan, 2009	All	Split of manual into VLTI general and MIDI specific part, therefore Sect. numbering changed.
83	31 Aug, 2008	All	Presence of off-axis guide star should be indicated in Phase 1, URLs updated for new ESO-web structure, parameters (wavelength solution, FINITO limits)
82	29 Feb, 2008	7.1	Updates for P82, brightness requirement for precision visibilities
81	29 Aug, 2007	all	Updates for P81, sensitivities
80	25 May, 2007	1.2, 6.5 8.1.4	Notes on FINITO Note on photometry frames

Issue	Date	Section/Parag. affected	Reason/Initiation/Documents/Remarks
80	1 March, 2007	All	Corrections in Sect. 1.2, 5, 6.5
79	31 August, 2006	All	Global revision for P79
78	26 June, 2006	All	Corrected again values of off-target guiding distance and limiting magnitude with ATs; new format; new paragraph (7.5) on observation constraints.
77	7 December, 2005	6.4	Paragraph on IRIS

Editors: Thomas Rivinius, Sébastien Morel, ESO Paranal Science Operations; [triviniu@eso.org](mailto:triviniu@eso.org)

# Contents

<b>1</b>	<b>INTRODUCTION</b>	<b>1</b>
1.1	Scope . . . . .	1
1.2	Acknowledgements . . . . .	1
1.3	Glossary . . . . .	1
1.4	Contacts . . . . .	2
<b>2</b>	<b>INTERFEROMETRY IN THE INFRARED</b>	<b>3</b>
2.1	Interferometric observables . . . . .	3
2.2	Visibility estimators . . . . .	4
2.3	Atmospheric transmission . . . . .	4
2.4	Background emission . . . . .	4
2.5	Atmospheric turbulence . . . . .	5
2.6	Conclusion . . . . .	6
<b>3</b>	<b>MIDI OVERVIEW</b>	<b>7</b>
3.1	A bit of history . . . . .	7
3.2	Optical Layout . . . . .	7
3.2.1	Cold optics . . . . .	7
3.2.2	Warm optics . . . . .	9
3.2.3	Dispersion . . . . .	10
3.3	Detector . . . . .	10
<b>4</b>	<b>MIDI IN PERIOD 89</b>	<b>12</b>
4.1	Acquisition . . . . .	12
4.2	Beam combination . . . . .	12
4.3	Spectral dispersion . . . . .	13
4.4	Fringe exposure . . . . .	14
4.4.1	Dispersed-Fourier mode . . . . .	14
4.4.2	Correlated Flux mode . . . . .	15
<b>5</b>	<b>THE VLTI ENVIRONMENT IN PERIOD 89</b>	<b>17</b>
5.0.3	Chopping . . . . .	17
5.1	Delay lines . . . . .	17
5.2	IRIS . . . . .	17
<b>6</b>	<b>PHASE-1 PROPOSAL PREPARATION WITH MIDI</b>	<b>19</b>
6.1	Target brightness . . . . .	19
6.2	Time of observation . . . . .	20
6.3	Geometry . . . . .	20
6.4	Guaranteed time observation objects . . . . .	21

6.5	Calibrator stars . . . . .	21
6.6	Observation constraints . . . . .	21
6.7	Visitor vs. service mode . . . . .	22
<b>7</b>	<b>MIDI OBSERVATIONS</b>	<b>23</b>
7.1	Observation sequence . . . . .	23
7.1.1	Target acquisition . . . . .	23
7.1.2	Fringe search . . . . .	24
7.1.3	Fringe measurement in Fourier mode . . . . .	24
7.1.4	Photometry . . . . .	24
7.2	Total sequence timing . . . . .	24
7.3	The VLT software environment for phase-2 . . . . .	25
7.4	Post-observation process . . . . .	25
7.4.1	Data handling . . . . .	25
7.4.2	The pipeline . . . . .	25
7.4.3	Data distribution . . . . .	26

## List of Figures

1	Principle of beam combination in long baseline interferometry. . . . .	3
2	Mid-Infrared atmospheric transmission . . . . .	5
3	Principle of MIDI optics. For simplicity, some of the mirrors are illustrated as lenses. . . . .	8
4	Lightpath in MIDI cold optics. . . . .	9
5	MIDI warm optics with individual elements labeled. . . . .	10
6	Image of dispersed fringes obtained in laboratory by MIDI with its grism. . . .	11
7	Dispersed-Fourier mode of MIDI. The white-fringe tracking is no longer used for observations. . . . .	15

## List of Tables

1	MIDI detector characteristics . . . . .	10
2	Characteristics of the MIDI filters. . . . .	13
3	Sensitivity limits for MIDI . . . . .	19

## List of Abbreviations

AT	Auxiliary Telescope
CS	Constraint Set
DIT	Detector Integration Time
DRS	Data Reduction Software
ESO	European Southern Observatory
FOV	Field Of View
FWHM	Full Width at Half Maximum
IRIS	Infra-Red Image Sensor
ISO	Infrared Space Observatory
MACAO	Multi-Application Curvature sensing Adaptive Optics
MIDI	MID-infrared Interferometric instrument
MIR	Mid-InfraRed
OB	Observation Block
OD	Observation Description
OPC	Observation Program Committee
OPD	Optical Path Difference
OPL	Optical Path Length
OS	Observation Software
OT	Observation Toolkit
P2PP	Phase-2 Proposal Preparation
QC	Quality Control
SM	Service Mode
SNR	Signal-to-Noise Ratio
STRAP	System for Tip-tit Removal with Avalanche Photodiodes
TSF	Template Signature File
USD	User Support Department
UT	Unit Telescope
VCM	Variable Curvature Mirror
VLT	Very Large Telescope
VLTI	Very Large Telescope Interferometer
VM	Visitor Mode

# 1 INTRODUCTION

## 1.1 Scope

This document summarizes the features and possibilities of the MID-infrared Interferometric instrument (MIDI) of the VLT, as it will be offered to astronomers for the six-month ESO observation period P89, running from 1 April 2012 to 30 September 2012.

The **bold** font is used in the paragraphs of this document to put emphasis on the important facts regarding MIDI in P89.

**This manual is intended to be used together with the VLTI user manual. The VLTI user manual contains important information on the VLTI subsystems relevant for MIDI observations.**

## 1.2 Acknowledgements

The editors thank Olivier Chesneau (Observatoire de la Côte-d'Azur, France) who wrote the very first version of this manual in August 2002, and also contributed to the update by providing us with some important MIDI facts after commissioning runs. The editors also thank Monika Petr-Gotzens, Andrea Richichi and Markus Wittkowski at ESO-Garching for their comments, as well as Markus Schöller and Andreas Kaufer at ESO-Paranal, and Jean-Gabriel Cuby (formerly at ESO-Paranal).

## 1.3 Glossary

### Constraint Set (CS)

List of requirements for the conditions (sky transparency, baseline...) of the observation that is given inside an **Observation block** (see below) which is only executed under this set of minimum conditions.

### Observation Block (OB)

The smallest schedulable entity for the VLT/VLTI. It consists of a sequence of **templates** (see below). Usually, one Observation Block includes one target acquisition and one or several templates for exposures.

### Observation Description (OD)

Sequence of templates used to specify the observing sequences within one or more OBs.

### Observation Toolkit (OT)

Tool used to create queues of OBs for later scheduling and possible execution.

### Proposal Preparation and Submission (Phase-1)

The phase-1 begins right after the Call-for-Proposal (CfP) and ends at the deadline for CfP. During this period, the potential users are invited to prepare and submit scientific proposals. For more information, see:

<http://www.eso.org/sci/observing/phase1.html>

### Phase-2 Proposal Preparation (P2PP)

Once proposals have been approved by the ESO Observation Program Committee (OPC), users are notified and the phase-2 begins. In this phase, users are requested to prepare their actual observations in the form of OBs, and to submit them electronically (in case of service



mode). The software tool used to build OBs is called the P2PP tool. It is distributed by ESO, and can be installed on the personal computer of the user. See:

<http://www.eso.org/observing/p2pp>

### **Service Mode (SM)**

In service mode (opposite of the “visitor mode”, see below), the observations are carried out by the ESO Paranal Science Operation (PSO) staff. Observations can be done at any time during the period, depending on the CS given by the user. OBs are put into a queue schedule in OT which later sends OBs to the instrument.

### **Template**

An elementary sequence of operations to be executed by the observation software (OS) of the instrument. The OS dispatches commands written in templates not only to instrument modules that control the detector and motors, but also to the telescopes and VLTI subsystems.

### **Template signature file (TSF)**

The file which contains input parameters for a template. Some of these parameters can be set by the user.

### **Visitor Mode (VM)**

The classical observation mode. The user is on-the-site to supervise his/her program execution.

## **1.4 Contacts**

The authors hope that this manual will help to get acquainted with the MIDI instrument before writing proposals, especially to scientists who are not used to interferometric observations. This manual is continually evolving and needs to be improved according to the needs of observers. If you have any question or suggestion, please contact the ESO User Support Department (<http://www.eso.org/sci/observing/>, email: [usd-help@eso.org](mailto:usd-help@eso.org)). The web page dedicated to the MIDI instrument is accessible at the following URL:

<http://www.eso.org/sci/facilities/paranal/instruments/midi/>

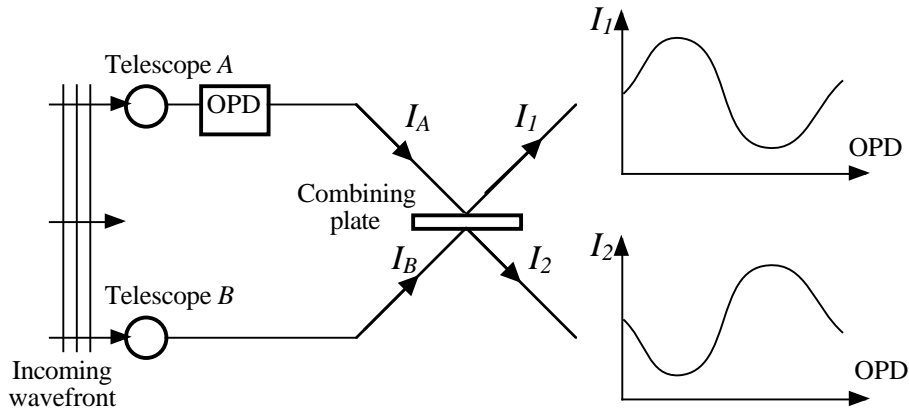


Figure 1: Principle of beam combination in long baseline interferometry.

## 2 INTERFEROMETRY IN THE INFRARED

### 2.1 Interferometric observables

An interferometer measures the coherence between the interfering light beams. The primary observable, at a given wavelength  $\lambda$ , is the complex visibility  $\Gamma = Ve^{i\phi} = \hat{O}(u, v)$ . In this expression,  $\hat{O}(u, v)$  is the Fourier transform of the object brightness angular distribution  $O(x, y)$ . The sampled point in the Fourier plane is  $(u = B_x/\lambda, v = B_y/\lambda)$ .  $(B_x, B_y)$  are the coordinates of the projected baseline.

$V$  corresponds to the “visibility”  $(I_{\max} - I_{\min})/(I_{\max} + I_{\min})$  of the fringes, its phase  $\phi$  is related to their position.

The visibility can be observed either as the fringe contrast in an image plane or by modulating the internal delay and detecting the consequent temporal variations of the intensity, as has always to be done in the case of coaxial beam combination. This latter mode is used in the MIDI instrument. In this case, the light from two telescopes A and B is combined by a half-transparent plate, and the combiner has two output channels 1 and 2 (Fig. 1). The total observed intensity is ideally given by:

$$\begin{aligned} I_1 &= I_{A1} + I_{B1} + 2V\sqrt{I_{A1}I_{B1}}\sin(2\pi\text{OPD}/\lambda + \phi) \\ I_2 &= I_{A2} + I_{B2} - 2V\sqrt{I_{A2}I_{B2}}\sin(2\pi\text{OPD}/\lambda + \phi) \end{aligned}$$

where  $I_1$  and  $I_2$  are the intensities from the two outputs of the combiner,  $I_{xy}$  the intensity from telescope  $x$  mixed for the channel  $y$  of the combiner, and OPD the path difference introduced by the atmospheric turbulence and by the optomechanical modulator (used to produce interferograms).

## 2.2 Visibility estimators

Due to atmospheric fluctuations the fringe pattern is usually in rapid motion, and the phase  $\phi$  of the complex visibility  $\Gamma$  cannot be estimated. It is often better to work with the square of the visibility  $V^2$  rather than  $V$  itself, because  $V^2$  estimators are less affected by the smearing of the moving fringe pattern. Averaging the squared visibility introduces a noise bias which however can be taken into account properly.

Performing a spectral dispersion of the output of a two-element pupil plane interferometer produces the so-called channelled spectrum (i.e., a fringe-modulated spectrum):

$$I(\sigma) = I_0(\sigma)[1 + V(\sigma) \cos(2\pi\text{OPD}\sigma) + \phi(\sigma)]$$

Here,  $\sigma$  is the wave number ( $1/\lambda$ ),  $I_0(\sigma)$  the spectrum of the light target and OPD, the total delay between the light path of the two telescopes. Note that the above equation corresponds to an ideal case for which no atmospheric turbulence would cause OPD fluctuation, and the incoming beams have the same intensity.

From this equation, we see that fringes with period  $\Delta\sigma = 1/\text{OPD}$  appear in the channelled spectrum, provided that  $I_0(\sigma)$  and  $\Gamma(\sigma)$  do not vary strongly with wavelength.

## 2.3 Atmospheric transmission

The thermal infrared (8 to 25  $\mu\text{m}$ ) atmospheric transmission is dominated by aerosol particles and by various molecular species, including  $\text{O}_3$  (9.6  $\mu\text{m}$ ),  $\text{CO}_2$  (14  $\mu\text{m}$ ), and  $\text{H}_2\text{O}$  ( $\leq 7$   $\mu\text{m}$ ), which absorb large parts of the infrared spectrum. Some of these components are constant for many hours at a time and over the whole sky, others may be variable on quite short time-scales or over short distances in the sky. Ground based mid-infrared observations can only be made in two atmospheric transparency “windows”, the N-band (wavelengths between 7.5 and 14  $\mu\text{m}$ ) and the Q-band (16 to 28  $\mu\text{m}$ ), but even in these windows the atmospheric absorption and radiation are a major disturbance. Nevertheless, new detector technology and the extremely dry mountain top of Cerro Paranal can improve the data quality. Transmission spectra are shown in Fig. 2.

## 2.4 Background emission

The atmosphere and telescope thermal radiation causes a high background that makes the observation of faint astronomical targets difficult. It is not unusual to observe objects which are thousands of times fainter than the sky. The mid-IR (8 to 15 $\mu\text{m}$ ) sky background is primarily due to thermal emission from the atmosphere i.e. it is equivalent to (1 - transmission) multiplied by a blackbody spectrum at a temperature of about 250K. The transmission (and therefore the emission) varies with atmospheric water vapor content and air mass.

On MIDI, the thermal background is dominated by 27 reflections (when the UTs are used, or 24 when the ATs are used) in the optical train at ambient temperature, which in combination give a 35% reflection and almost radiate like a blackbody. The thermal background therefore is dependent on the sky and interferometer temperature (lower in winter for instance) and also on possible dust particles on the numerous mirrors used to relay the beams.

Under these conditions, it has become a standard procedure to observe the target (together with the inevitable sky) and subtract from it an estimate of this sky background obtained by

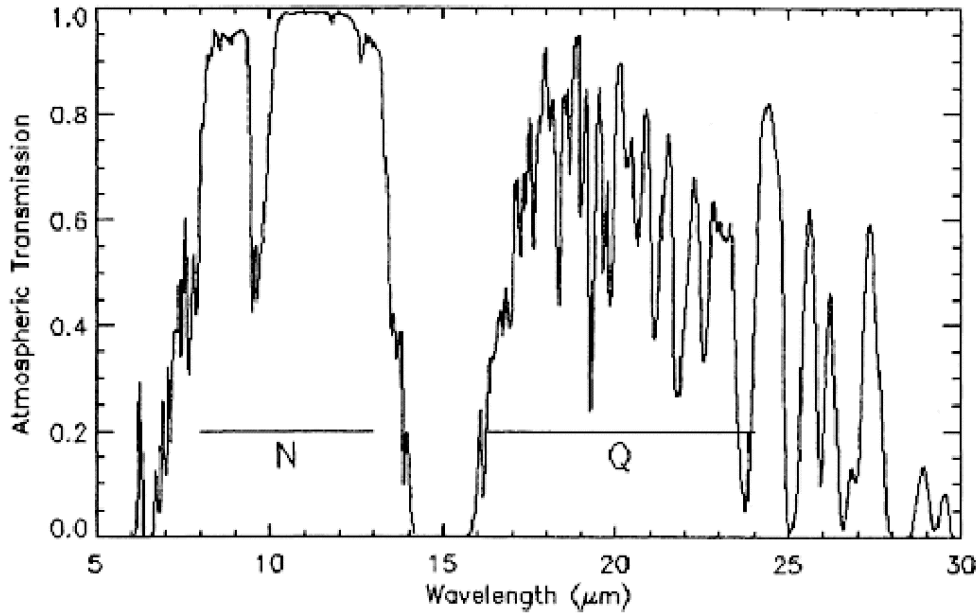


Figure 2: Mid-Infrared atmospheric transmission

fast switching between target and an empty sky position. The method used with MIDI to deal with this correction is called “chopping”. The characteristic time of such a correction is dependent on the sky variability (which is fast), and on the weather. Sky subtraction has the additional advantage that detector artifacts are removed.

In interferometric setup without the photometric channels, chopping is not employed. To cancel out the background, we rely on the fact that between the interferometric channels of MIDI, the background is almost totally correlated, whereas the interferometric signals are in phase opposition. Subtracting in each detector frame the area illuminated by one interferometric channel from the area illuminated by the other will therefore cancel out the thermal background in the frame.

## 2.5 Atmospheric turbulence

Atmospheric turbulence is a major contributor to the difficulty of optical and infrared interferometry from the ground. Rapid atmospheric variations of the OPD between the two arms of an optical or infrared interferometer, if uncorrected, will cause a smearing of the fringe pattern and a strong decorrelation of the observed signals. The correlation time of the atmosphere is milliseconds in the visible and increases to hundreds of milliseconds in the mid-IR.

“Seeing” is the historical term for the fact that the image produced by a telescope, which is larger than approximately ten centimeters (in optical), is not as sharp as one would expect from its size and optical quality, but is fuzzy. The fuzziness changes with time and weather conditions. A short exposure (milliseconds) of such an image reveals a large number of “speckles”. These speckles move around, disappear and reappear on short time-scales. The speckle image is in fact a result of interference between wavefronts of randomly appearing, moving, and disappearing sub-apertures. These sub-apertures are defined by the atmospheric turbulence “bubbles” in the first few tens to hundreds of meters above the telescope.

The sensitivity of interferometers strongly depends on the seeing, i.e. on the Fried param-

eter, defined as follows: the resolution of seeing-limited images obtained through an atmosphere with turbulence characterized by a Fried parameter  $r_0$  is the same as the resolution of diffraction-limited images taken with a telescope of diameter  $r_0$ . Observations with telescopes much larger than  $r_0$  are seeing-limited, whereas observations with telescopes smaller than  $r_0$  are essentially diffraction-limited. The scaling of  $r_0$  with wavelength is favorable for MIDI since:

$$r_0 \propto \lambda^{\frac{6}{5}}$$

which at 10  $\mu\text{m}$  and for a 0.8-arcsec seeing in the visible leads to  $r_0 = 4.6$  m. It is therefore much easier to achieve diffraction-limited performance at longer wavelengths, and simple tip-tilt correction already will give correct results with large apertures. An interferometer correctly works only if the wavefronts from the individual telescopes are coherent (i.e., have phase variances not larger than  $\approx 1$  rad<sup>2</sup>).

Scintillation is another consequence of inhomogeneities in the atmosphere at altitudes of some kilometers. Phase gradients due to the pressure gradients of the turbulent air cause mild deflections of the direction of travel of the wavefront. The cross section of the resulting cone of rays, intercepted by the telescope pupil, is at any time brighter or fainter than the average intensity (the “cylinder of rays” that would ideally feed each telescope in absence of turbulence). Scintillation is less important in the mid-infrared where fluctuations of sky emission (“sky noise”) dominate.

## 2.6 Conclusion

These observational difficulties, mostly resulting from high background variations, have led to the development of specific observation techniques. These techniques are included in the templates (see Sect. 1.3) that are used to control MIDI and the telescopes. The templates are extensively described in the template manual, available from the MIDI webpage at beginning of phase-2 proposal preparation for P89.

## 3 MIDI OVERVIEW

### 3.1 A bit of history

MIDI belongs to the first generation of VLTI instruments. Conceptual studies for a VLTI mid-infrared instrument started in 1997. The Final Design Review of MIDI was passed in early 2000 for the hardware, and mid-2001 for the software. The integration took place at the Max-Planck Institut für Astronomie, Heidelberg (Germany). After Preliminary Acceptance in Europe in September 2002, MIDI was shipped to Paranal and re-assembled there in November 2002, where it obtained its first fringes with the UTs on the 12 December 2002. Since 1 September 2003, MIDI is offered to the worldwide community of astronomers, for observations in service mode or in visitor mode.

The MIDI consortium, who built and commissioned MIDI, consists of several european institutes: Max Planck Institut für Astronomie, Heidelberg (Germany); Netherlands Graduate School for Astronomy (NOVA), Leiden (The Netherlands); Department of Astronomy, Leiden Observatory (The Netherlands); Kapteyn Astronomical Institute, Groningen (The Netherlands); Astronomical Institute, Utrecht University (The Netherlands); Astronomical Institute, University of Amsterdam (The Netherlands); Netherlands Foundation for Research in Astronomy, Dwingeloo (The Netherlands); Space Research Organization Netherland, Utrecht and Groningen (The Netherlands); Thüringer Landessternwarte, Tautenburg (Germany); Kiepenheuer-Institut für Sonnenphysik, Freiburg (Germany); Observatoire de Paris-Meudon, Meudon (France); Observatoire de la Côte d'Azur, Nice (France).

### 3.2 Optical Layout

Inside MIDI, the beam combination occurs in a plane close to the re-imaged pupil, and the signal is detected in an image plane (infinity).

MIDI in the interferometric laboratory is composed by two main parts: the warm optics on the MIDI table and the cold optics in the cryostat. In addition, in the adjacent Combined Coudé Laboratory, are located an infrared CO<sub>2</sub> laser (used for calibration measurements), the control electronics and the cooling system.

#### 3.2.1 Cold optics

Since radiation at 10  $\mu\text{m}$  is dominated by thermal emission from the environment, most of the instrument optics has to be in a cryostat and to be cooled to cryogenic temperatures (6 K to 12 K for the detector,  $40\pm 5$  K for the cold bench, 77 K for the outer radiation shield).

In the cryostat, the elements of the cold optics appear in the following sequence along the beams:

1. Shutter
2. Cold pupil stops
3. First off-axis paraboloids (M1)
4. Diaphragms in intermediate focus (spatial filters)

### Principle of MIDI - the MID- infrared Interferometer for the VLTI

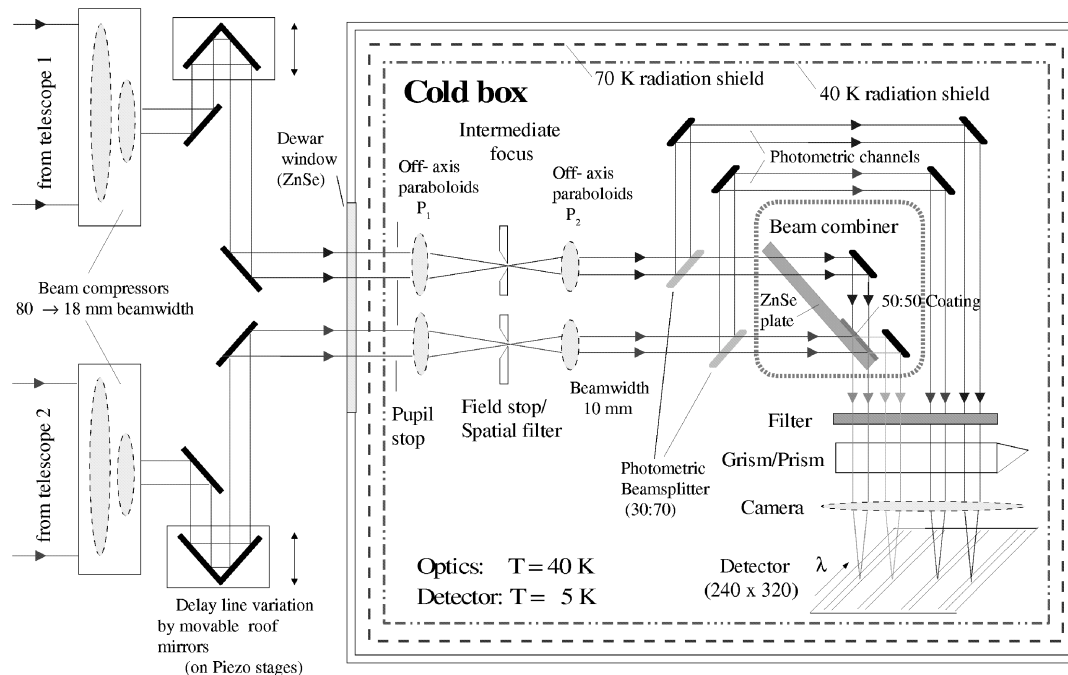


Figure 3: Principle of MIDI optics. For simplicity, some of the mirrors are illustrated as lenses.

5. Second off-axis paraboloids (M2)
6. Folding flat mirror (M3)
7. Photometric beam splitter plates
8. Folding flat mirrors (for one of the photometric channels) (M4 and M5)
9. Beam combiner (beam combiner plate, M6 and M7)
10. Filters
11. Dispersive elements (prism, grism)
12. Cameras
13. Detector

The core of the cold optics is formed by the beam combiner. It consists of a half-transparent plate on which the telescope beams are superimposed: Nominally 50% of beam A being transmitted and nominally 50% of beam B being reflected into a common path. The remaining light, 50% reflection of beam A and 50% transmission of beam B, is superimposed, too, and directed towards the detector with an extra mirror. In addition, the cold optics offers the possibility to extract a signal from the beams before combination (by the mean of cold optics beamsplitters), in order to get the photometric information (see Fig. 4). The intensity extracted by the “photometric” beamsplitters for each beam is around 30% of the incoming intensity.

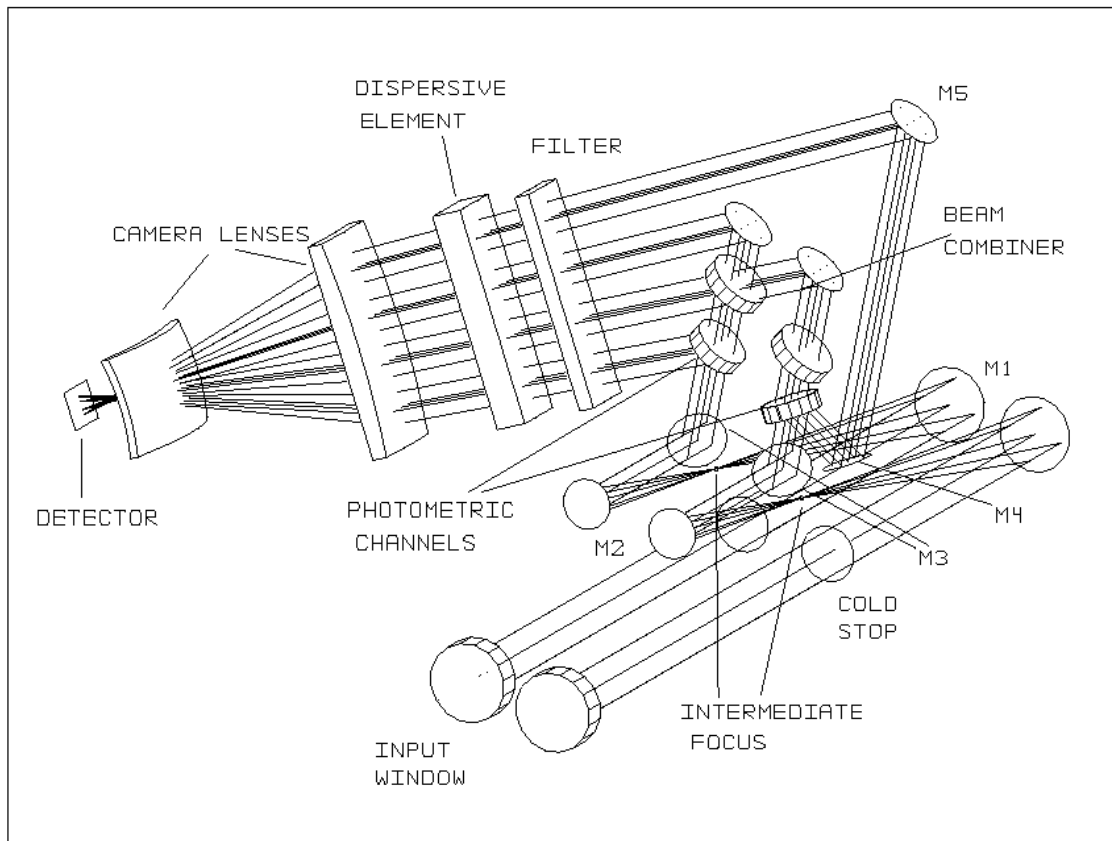


Figure 4: Lightpath in MIDI cold optics.

MIDI has two focusing mechanisms: the first one actuates the M1 mirrors to focus the beams on the spectroscopy slits (if dispersion is used) or on future spatial filters, and the second one translates the detector plane to bring it at the focus of the “camera” (germanium set of lenses). Baffling within the instrument is mainly done by a cold pupil stop just downstream of the entrance window of the cryostat.

### 3.2.2 Warm optics

OPD modulation is performed in the ambient-temperature laboratory environment. An overview on this so-called “warm optics” is given in Fig. 5. As said above, the degree of coherence of the light target (i.e. the object visibility at the actual baseline setting) is measured by stepping the internal OPD rapidly over at least one wavelength within a time when the fringe has not moved more than  $1 \mu\text{m}$  on the average ( $t < 0.1\text{s}$ ). This operation is performed by two dihedral mirrors mounted on piezo translators (DLA and DLB, one for each arm). One piezo is used for OPD modulation. A translation stage underneath one of them (DLA) allows to change the internal OPD by a larger amount.

As sketched by Fig. 5, the warm optics bench also includes ancillary devices for calibration and alignment that can be inserted in the optical path. These devices are beamsplitter and feeding optics for a  $\text{CO}_2$  test laser ( $\lambda=10.6 \mu\text{m}$ ), spatially-incoherent blackbody target, and alignment target plates.



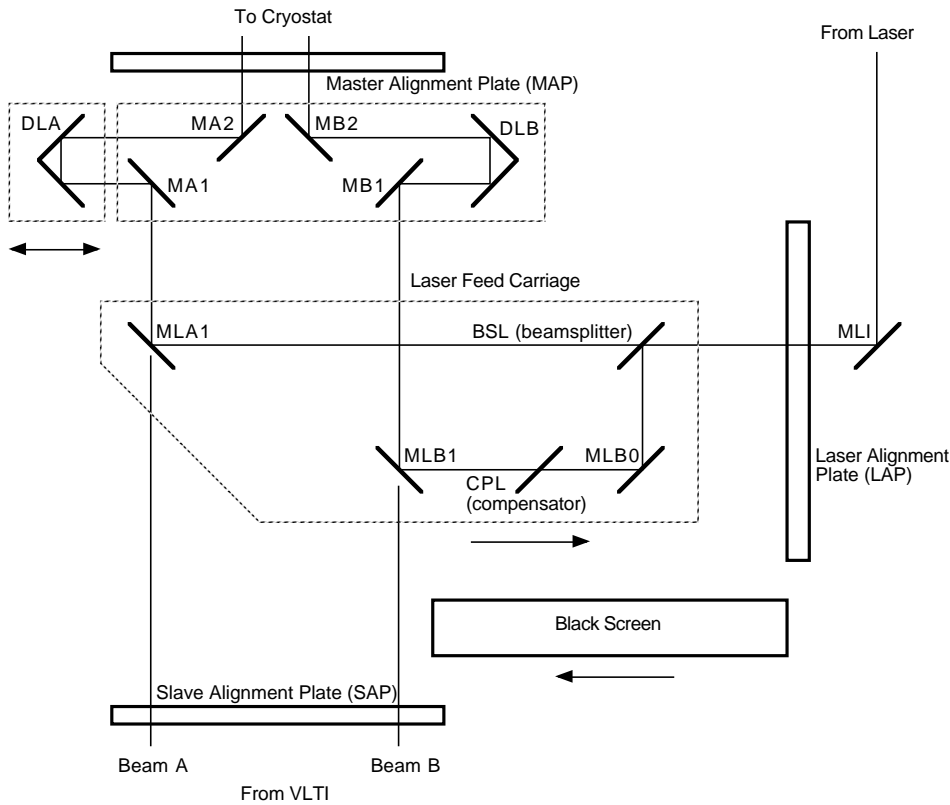


Figure 5: MIDI warm optics with individual elements labeled.

### 3.2.3 Dispersion

MIDI has a spectroscopic mode based on either a NaCl prism or a KRS5 grism, that are used along with beam combination. The interest of such a mode, besides the possibility to measure fringe visibility for different spectral channels in the N-band, is explained in Sect. 4.3.

## 3.3 Detector

The detector is a  $320 \times 240$ -pixel Raytheon Si:As Impurity Band Conduction (IBC) array (also called “BIB”, blocked impurity band). The detector characteristics are summarized in Table 1.

Table 1: MIDI detector characteristics

Array dimensions	$320 \times 240$
Pixel Size	$50 \mu\text{m} \times 50 \mu\text{m}$
Peak Quantum efficiency	34%
Dark current per pixel	$10^4 \text{ e}^-/\text{s}$ at 10 K
Operating temperature	4 to 12 K
Well capacity	$1.1 \times 10^7 \text{ e}^-$
RON	$\approx 800 \text{ e}^-$

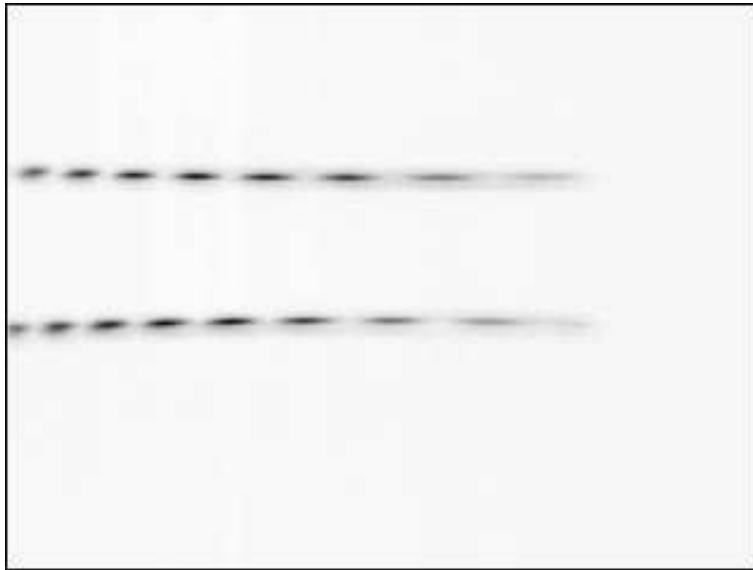


Figure 6: Image of dispersed fringes obtained in laboratory by MIDI with its grism.

The standard operating mode of the detector is called “Integrate-Then-Read” (ITR). In this “snapshot” mode a reset is performed simultaneously on the whole chip before the start of integration. The end of integration is set by applying a bias voltage that inhibits further accumulation of signal. The frame rate in “snapshot” mode is determined by the sum of the integration time and the readout time.

ITR mode allows to select an integration as short as 0.2 ms per frame. The minimum integration time is given by the time needed to propagate the reset signal. The time required to readout a full frame in ITR mode is about 6 ms. However, in many cases there is no need to read out the full detector array: it may be advantageous to use sub-array readout (windowing). Windowing of the detector by line selection reduces the time needed for readout (hardware windowing). Software windowing by column selection after readout reduces the amount of data to be processed in the downstream steps of data handling.

Fig. 6 shows the type of data that is collected by MIDI if a dispersive element is inserted in the optical path after the beam recombination: dispersed fringes with phase opposition from the two recombined beams, in the image plane.

## 4 MIDI IN PERIOD 89

MIDI combines many aspects that usually exist independently in several astronomical instruments. This includes visibility measurements (interferometry), spectral dispersion (spectroscopy), imaging with a detector array (imaging) and background level plus fluctuation measurement (thermal infrared imaging techniques). Hence, MIDI offers a large possibility of setups selectable by the user.

For P89, the available setups consist of:

- **Acquisition:** imaging mode, several spectral filters available.
- **Beam combination:** “HIGH\_SENS” (high-sensitivity): no simultaneous photometric channel), or “SCI\_PHOT” (science with photometry): simultaneous photometric channels, “CORR\_FLUX” (correlated flux): no photometry on target, just on calibrators.
- **Fringe type:** dispersed (normal)
- **Spectral mode:** prism or grism, with 200- $\mu\text{m}$  (0.52 arcsec on sky with UTs, 2.29 arcsec with ATs) slit.
- **Detector readout:** integrate-then-read.
- **Fringe exposure:** Fourier mode (long scan) with dispersion, self fringe-tracking.

The Integrate-Then-Read mode has been introduced in detail in Sect. 3.3. In the following details about the modes for the beam combiner, the dispersive element and the fringe exposure are described.

### 4.1 Acquisition

As a rule, IRIS (see Sect. 5.2) is used for acquisition. If IRIS cannot be used or the user specifically requests a MIDI acquisition image for scientific purpose, the MIDI imaging mode will be used for acquisition instead (or in addition). The imaging mode requires the selection of a spectral filter.

The “N8.7” (N-band short wavelengths) filter normally yields the best signal-to-noise ratio in the exposures obtained from acquisition. Nevertheless, the user has the possibility to select the filter for the acquisition. This is important if, for example, the target shows strong absorption around 8.7  $\mu\text{m}$ . Table 2 gives the characteristics of these filters. More data (transmission vs. wavelength plots and ASCII tables) are available from:

<http://www.eso.org/sci/facilities/paranal/instruments/midi/inst/filters.html>

### 4.2 Beam combination

As already explained in Sect. 3.2.1, the high sensitivity beam combination (HIGH\_SENS) is realized by using the  $R/T = 50/50$  combining plate alone. In order to obtain photometric information, exposures with one beam only (first A then B) through the beam combiner with the same optical path are recorded after the fringe observation has been performed.

The SCLPHOT setup uses the same combining plate as HIGH\_SENS, but two beamsplitting plates with  $R/T \approx 30/70$  are inserted in the optical path of each beam before it reaches the combining plate, in order to extract the photometric signal.

### 4.3 Spectral dispersion

Because of the domination of the thermal background in detector frames, it is necessary to spread the incoming light onto a large zone of the detector, to increase the DIT (detector integration time) without saturating the pixels. The sampling time of one fringe has, however, to be adjusted to stay within the atmospheric coherence time at  $10 \mu\text{m}$  (100 ms typically). Respecting this rule, it has been noticed that fringe dispersion on MIDI yields a better sensitivity than undispersed fringes.

Obviously, dispersion in interferometry allows visibility calculation for different spectral channels. In this case, the minimum fringe signal for each spectral channel must be, more or less, equivalent to the limiting correlated magnitude yielding a visibility over the whole N-band (see Sect. 7.1).

The estimated spectral resolution  $\lambda/\Delta\lambda$  of the prism is  $R = 30$  (at  $\lambda = 10.6 \mu\text{m}$ ). The relationship between wavelength (in micron) and detector pixel on MIDI with the prism is given by:

$$\lambda = C_2 X^2 + C_1 X + C_0$$

where  $X$  is the pixel position (1 = left edge column, 320 = right edge column in the displayed image). The coefficients are:

$$\begin{aligned} C_2 &= -0.0001539 \\ C_1 &= 0.009491 \\ C_0 &= 15.451905 \end{aligned}$$

The accuracy of the above formula with these coefficients is  $0.2 \mu\text{m}$ . Future MIDI calibrations should further refine these values.

The estimated spectral resolution  $\lambda/\Delta\lambda$  of the grism is  $R = 230$  (at  $\lambda = 10.6 \mu\text{m}$ ). Its  $C_0$ ,  $C_1$ , and  $C_2$  coefficients (see above for definition) are:

Table 2: Characteristics of the MIDI filters.

Name	Central wavelength ( $\mu\text{m}$ )	FWHM ( $\mu\text{m}$ )
Nband	10.34	5.24
SiC	11.79	2.32
N8.7	8.64	1.54
[ArIII]	9.00	0.13
[SIV]	10.46	0.16
[NeII]	12.80	0.21
N11.3	11.28	0.60

$$\begin{aligned}
C_2 &= -1.21122 \times 10^{-6} \\
C_1 &= 0.0232192 \\
C_0 &= 6.61739
\end{aligned}$$

The accuracy of the above formula with these coefficients is  $0.05 \mu\text{m}$ . Future MIDI calibrations should refine these values.

In spectral dispersion, a slit is inserted in the intermediate focus inside the cold-optics of MIDI. The width of this slit is  $200 \mu\text{m}$ , which corresponds to  $0.52$  arcsec on sky with the 8-m unit telescopes, and to  $2.29$  arcsec on sky with the 1.8-m auxiliary telescopes.

It is important to notice that the prism and the grism setups use different cold cameras, providing different magnification factors on the detector:

- Prism mode: “Field” camera (as for image acquisition), magnification= 3 pixels per  $\lambda/D$  ( $1 \lambda/D = 0.26$  arcsec on sky with UTs,  $1.14$  arcsec with ATs).
- Grism mode: “Spectral” anamorphic camera, magnification= 2 pixels per  $\lambda/D$  along the y-axis, and 1 pixel per  $\lambda/D$  along the x-axis (dispersion direction).

## 4.4 Fringe exposure

In P89, only the classical “dispersed-Fourier Mode” mode is offered.

### 4.4.1 Dispersed-Fourier mode

In dispersed-Fourier mode (Fig. 7), fringes are scanned over an OPD that is several  $\bar{\lambda}$  long, to get interferograms (fringe packets) showing the main lobe of the coherence envelope. As the background is strongly correlated between the two interferometric channels, subtraction will cancel the background and enhance the interferometric signal (fringes are shifted by  $\pi$  between the two recombined beams). The signal obtained for one scan (if the OPD has been compensated to allow fringe detection) is the actual interferogram. Since self fringe tracking is used, the zero-OPD point is computed in real-time by MIDI for each scan, and then converted into an offset sent to the tracking delay line. In dispersed-Fourier mode, we now systematically use group-delay tracking: the OPD is measured from the position of a fringe peak in the Fourier transform of the frame showing dispersed fringes. Scanning the OPD remains necessary to determine the OPD sign, and also to provide a better quality of the visibility in each spectral channel at data reduction time.

A raw (uncalibrated) visibility estimation requires a few hundred scans.

**The parameters for fringe measurement in dispersed-Fourier mode in P89 are the following (indicative values and subject to minor changes):**

- Dispersion by either prism or grism (see Sect. 4.3).
- One (1) detector frame per OPD sample.
- Five (5) OPD samples for fringe.

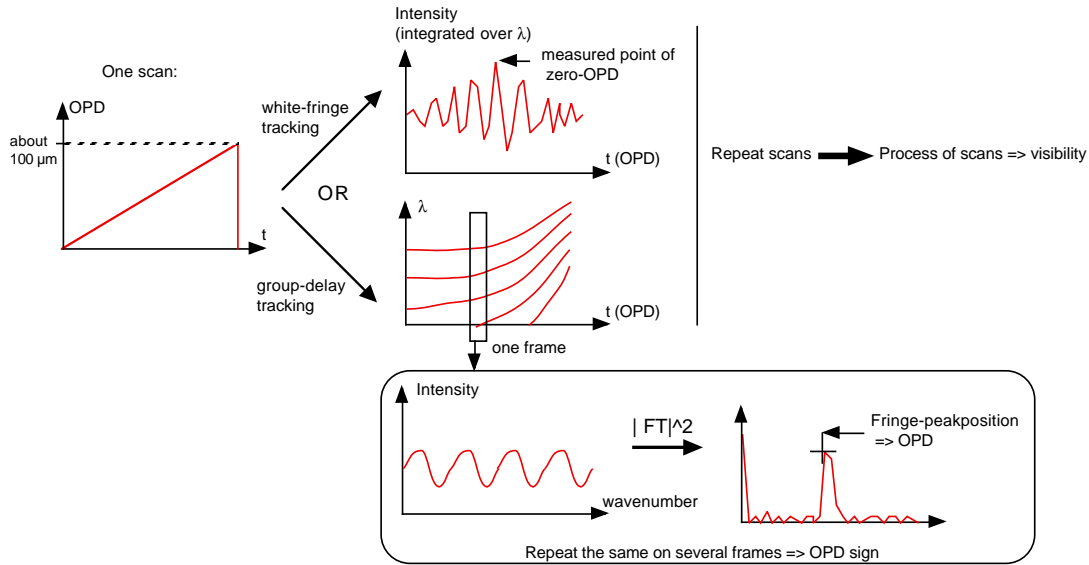


Figure 7: Dispersed-Fourier mode of MIDI. The white-fringe tracking is no longer used for observations.

- 8 fringes per scan ( $\Rightarrow$  OPD scanning range= 80  $\mu\text{m}$ ).
- Zero OPD offset (0 or 50  $\mu\text{m}$ ).

After completion of the exposure, each interferogram can be individually processed by Fourier transform to yield a raw visibility. The algorithm used for this computation usually involves a Fourier transform of the interferograms, hence the name of this fringe mode.

#### 4.4.2 Correlated Flux mode

In HIGH\_SENS or SCIPHOT mode source photometry is taken simultaneously or immediately after the fringe track. Due to the background being fully correlated, i.e. subtractable in the fringe exposure without residuals, photometry is harder to obtain at good quality than fringes. This is the effective limiting factor in the modes relying on photometry to calibrate data. Under certain conditions, this limitation can be worked around by obtaining fringes on the source only, i.e. the measured correlated flux, and comparing them to the measured vs. the known correlated flux of the calibrator. This way the calibrated correlated flux of the source can be determined.

An observing sequence to obtain a correlated flux with MIDI consists of a calibrator observation (with photometry), a science source observation (without photometry), and again the same calibrator (with photometry). This means that the science target can be as faint as the MIDI fringe tracking limit, which is 0.2 Jy at the UTs, but the calibrator must be brighter than the PRISM/HIGH\_SENS UT limit of 1 Jy. The use of the same calibrator for all correlated flux measurements of a given target eliminates potential problems due to not well determined calibrator fluxes.

In order to compare the correlated target fluxes to each other, which is necessary to infer target geometry, as they are not absolutely calibrated file visibilities, the target must not be variable on timescales similar or shorter than the temporal separation of the observation.

Since faint targets at 0.2 Jy cannot be acquired with MIDI itself, correlated flux mode targets have to be sufficiently bright in K-band to be acquirable with IRIS.

This mode is currently offered for UTs and in visitor mode only.

## 5 THE VLTI ENVIRONMENT IN PERIOD 89

This section only deals with aspects of the VLTI that are unique to MIDI observations. For a complete overview see the VLTI user manual.

### 5.0.3 Chopping

Performing mid-IR observations requires to discriminate the faint stellar signal against a strong and variable background that mostly comes from the sky and optical train thermal emission (see Sect. 2.4). The standard technique consists in moving the secondary mirror of the telescope (M2) at a rapid frequency (of the order of one Hertz for the VLTI). The maximum chopping throw of a UT is 30 arcsec, more than needed for the 2-arcsec interferometric field of the VLTI.

Chopping against an empty part of the sky reduces the background signal to zeroth order and normally removes the temporal background variations. An intensity gradient, sometimes strong, remains in the background-subtracted data. It is due to the light paths through the system which are slightly different for the “on” and “off” positions.

Chopping is always used for MIDI image acquisition (to perform the beam overlap), but not during fringe exposure in “HIGH\_SENS” setup. **The power spectrum of the background variations should not affect the fringe visibility down to the offered limiting magnitude (1 Jy in service mode with the prism and HIGH\_SENS beam-combiner for the UTs).**

### 5.1 Delay lines

The VLTI delay lines are based on a cat’s eye optical design featuring a variable curvature mirror (VCM) at its center. The aim of the VCM is to perform a pupil transfer to a desired location, whatever the delay line position. In the case of MIDI, the optimal pupil position is the “cold stop” that is located inside the cryostat after the shutter. The advantages of transferring the pupil are:

- An optimized field of view (For precise parameters see the VLTI manual). Fringes can be obtained from any target within the FOV.
- A reduction of the thermal background related to VLTI optics.

Although VCMs are installed on all delay lines and are likely to be used, In P89, we *guarantee* that the VCMs are used for MIDI observations with the **ATs only**.

### 5.2 IRIS

IRIS is the infrared field-stabilizer of the VLTI. Next to other advantages explained in the VLTI-manual, IRIS allows to skip the acquisition by MIDI imaging, reducing considerably the execution overheads. If the target is too faint for IRIS, then the acquisition by MIDI will be executed. Users still have to indicate which MIDI filter has to be used for acquisition, but it does not mean that MIDI acquisition exposures will be taken.



As a rule, we do not guarantee that MIDI acquisition images are taken in normal operation. However, acquisition images with MIDI can specifically be requested by the user at phase 2, if they are to be used for scientific purposes.

## 6 PHASE-1 PROPOSAL PREPARATION WITH MIDI

Submission of proposals for MIDI must be done using the ESIFORM LaTeX template. It is important to carefully read the following information before submitting a proposal, as well as the ESIFORM user manual. The ESIFORM package can be downloaded from:

<http://www.eso.org/sci/observing/proposals/esoform.html>

Considering a target which has a scientific interest and for which MIDI could reveal interesting features, the first thing to do is to determine whether this target can be observed with MIDI or not. Several criteria must be taken into account.

### 6.1 Target brightness

The brightness of the target in the N-band will determine whether it is observable at all in self fringe-tracking mode, and whether meaningful photometry data can be obtained, or only correlated flux can be measured. **The limiting magnitudes for MIDI observations on unresolved objects in P89 are the following:**

Table 3: Sensitivity limits for MIDI

Telescopes	Beam combiner	Dispersion	Limiting N-mag.	Equiv. in Jy@12 $\mu$ m
UT	CORR_FLUX	PRISM	5.7	0.2
UT	HIGH_SENS	PRISM	4	1
UT	HIGH_SENS	GRISM	2.8	3
UT	SCLPHOT	PRISM	3.2	2
UT	SCLPHOT	GRISM	2	6
AT	HIGH_SENS	PRISM	0.74	20
AT	HIGH_SENS	GRISM	0.31	30
AT	SCLPHOT	PRISM	0.0	40
AT	SCLPHOT	GRISM	-0.44	60

The correlated flux (CF) is defined by the uncorrelated flux (PF, for photometric flux) multiplied by the estimated visibility, i.e. the product brightness  $\times$  visibility. Extended objects might be well above these limits for uncorrelated flux, but have correlated fluxes below them. In such cases, i.e. when only the CF is below the limiting magnitude for the mode, but still above the fringe-tracking limit (see correlated flux mode for UTs, for ATs the limit is estimated by  $CF = 0.5 \times PF$ ), observations will be moved to visitor mode, as such observations usually require real-time decisions on observing strategy.

All service observing modes rely on IRIS for acquiring the target, and thus must not be fainter than the IRIS limiting magnitude (see the VLTI manual). If the target is invisible in IRIS, but above the PF flux limit, it can only be done in visitor mode, including the additional acquisition overhead (see 7.2).

Still, even a bright target may be so extended, and therefore has such a low visibility that no fringe tracking is possible on it. In this case MIDI cannot observe it.

The visual brightness will determine whether MACAO or STRAP can be used on the target or not, details are found in the VLTI user manual.

Highest achievable precision for calibrated visibilities require observations taken in SCI-PHOT mode, with both target and calibrator brighter than 15 Jy with the UTs and 200 Jy with the ATs. We recommend to observe SCI-CAL-SCI sequences (see next Sect.) for high precision purposes.

In general it is not advisable to have calibrator fluxes too close to the limit of the respective mode. For the sake of a robust calibration, in particular photometrically, we recommend calibrator fluxes at least 1.5 times higher than the limit for photometry.

## 6.2 Time of observation

In P89 25 minutes are the estimated execution time per OB, regardless of the correlated magnitude in N-band of the target, and both for science and calibrator. If the user requests a single calibrator per science target (SCI-CAL), **slots of 50 minutes per calibrated visibility vs. wavelength curve at a given  $(u, v)$  point, will be allocated.** If the user requests two calibrator observations per science target (CAL-SCI-CAL sequence), **slots of 75 minutes will be allocated.**

For certain visitor mode programs, in particular for targets very close to the limit of MIDI, or too faint for IRIS, and otherwise challenging acquisitions, a value of 80 minutes per calibrated visibility point (SCI-CAL) has turned out to be more realistic, and the user is requested to state such circumstances in the proposal in order to ensure a proper time allocation.

Since the DIT (detector integration time) of MIDI is usually determined by the level of the thermal background illuminating the detector, the user will have no freedom on this parameter. Paranal Science Operations can adjust parameters of fringe exposures for faint objects, but will do so only during VM observations on request of the visiting astronomer at the console. The values of these parameters (which are not visible for the user from the templates) are included in the FITS header of the data files that will be delivered to the user after observation.

## 6.3 Geometry

Important parameters of the instrument to be taken into account for the preparation of the observing schedule are the VLTI geometry during observation, the  $(u, v)$  coverage. The selection of the baseline requires the knowledge of both the geometry of the VLTI and of that of the target.

**To assess observability of a target with VLTI, it is mandatory to use the VisCalc software.** The front-end of VisCalc is a comprehensive web-based interface. VisCalc can be used from any browser from the URL:

<http://www.eso.org/observing/etc>

It is important to check that the altitude of the object is not below  $30^\circ$  during the observations, which is the operational limit of the VLTI.

Since we had problems in service mode in the past with over-resolved targets (which appeared resolved in imaging mode at the acquisition, or for which no fringes were found), or with low-precision IR coordinates (which could not be seen on MIDI), we encourage the users to collect as much information on their targets as possible before submitting a MIDI proposal. For instance, a proposal for a pre-imaging study on VISIR (VLT instrument) may help to know more about the feasibility on MIDI.

## 6.4 Guaranteed time observation objects

proposers must check any scientific target against the list of guaranteed time observation (GTO) objects. Only the GTO consortium is allowed to observe these objects with MIDI. The GTO target list is submitted every period individually.

To make sure that a target has not been reserved already for P89, the list of GTO objects can be downloaded from:

<http://www.eso.org/sci/observing/visas/gto/>

## 6.5 Calibrator stars

High quality measurements require that the observer minimizes and calibrates the instrumental losses of visibility. To get a correct calibration, the user should use appropriate calibrator stars in terms of target proximity, calibrator magnitude *and* apparent diameter. In the case of MIDI, two calibration sequences are offered. In the SCI-CAL sequence the calibrator is, as a rule, observed after the science target, using the same templates. Exceptionally, the calibrator may be observed before for operational reasons, e.g. when the target is faint and pupil alignment is a mandatory step, like after a baseline change. Alternatively, the user can request a CAL-SCI-CAL sequence, where the science observation is sandwiched between calibrator observations.

**For each science target, a calibrator star must be provided by the user with the submission of the phase-2 material.** To help the user to select a calibrator, a tool called “CalVin” is provided by ESO. CalVin can be used from any web browser. Like VisCalc, CalVin can be used on the web from:

<http://www.eso.org/observing/etc>

The users have also the possibility to use spectrophotometric calibrators as calibrators of their targets, if they wish to later perform a calibration of the correlated flux. A list of spectrophotometric calibrators (MIDI-consortium calibrators that are also referenced in the ISO catalogs) is available at:

[http://www.eso.org/sci/facilities/paranal/instruments/midi/tools/spectrophot\\_std.html](http://www.eso.org/sci/facilities/paranal/instruments/midi/tools/spectrophot_std.html)

The standard observation consists of a SCI-CAL pair. The additional time for the CAL-SCI-CAL sequence has to be included in the phase 1 proposal.

## 6.6 Observation constraints

The **Moon** constraint is irrelevant for mid-IR observations. However, if the Moon is too close to the target, the scattered moonlight may prevent adaptive optics from working correctly. The VLTI astronomers make sure that the OBs in service mode are executed when the Moon is far enough from the targets. In visitor mode, users should carefully schedule their night-time using Moon ephemeris to avoid problems of scattered moonlight.

The **seeing** condition has no impact on the MIDI image quality: as long as the seeing and the  $\tau_0$  allow madaptive optics correction, the MIDI images are diffraction-limited.

The **sky transparency** constraint is relevant only in special cases: in HIGH\_SENS mode, thin cloud conditions may cause variations of flux between fringe-track and photometry exposures. Also, if a faint off-axis guide star is used, thin cloud conditions may have impact on the MIDI image quality. On the other hand, thin cloud conditions are not a problem in SCI\_PHOT mode if the guide star is brighter than  $V = 15$  (if the UTs are used) or  $V = 12$  (if the ATs are used). The difference between photometric and clear conditions are irrelevant for MIDI operations.

## 6.7 Visitor vs. service mode

**For P89, MIDI is offered in service mode and in visitor mode (see Sect. 1.3).** For the phase-1 of a period, the unique contact point at ESO for the user is the User Support Department (see Sect. 1.4). For the phase-2, USD is still the contact point for service mode, and the Paranal Science Operation department is the contact point for visitor mode ([http://www.eso.org/sci/facilities/paranal/sciops/VA\\_GeneralInfo.html](http://www.eso.org/sci/facilities/paranal/sciops/VA_GeneralInfo.html)).

**The visitor mode observations are likely to be required for proposals adopting non-standard or complicated observation procedures**, for instance complex structures in the field-of-view of MIDI. The OPC will decide whether a proposal should be observed in SM or VM. As for any other instrument, ESO reserves the right to transfer visitor programs to service and *vice-versa*.

## 7 MIDI OBSERVATIONS

Once a MIDI proposal is accepted by the OPC, it must be set in a form that it can be carried out by Paranal Science Operation. Some knowledge of the observation sequence of MIDI is necessary before tackling phase-2.

### 7.1 Observation sequence

An observation with MIDI in P89 can be split in the several subtasks:

1. Slew telescopes to target position on sky, and slew one of the delay-lines to the expected zero-OPD position. Bring them in “tracking” state (pre-defined sidereal trajectory).
2. Bring telescopes in Nasmyth (UT only), then Coudé (MACAO or STRAP) guiding mode (use of a guide star for field stabilization).
3. Adjust telescope positions, so the beams from the target will overlap inside MIDI and be recombined.
4. Search the optical path length (OPL) offset of the tracking delay line yielding fringes on MIDI (actual zero-OPD), by OPD scans at different offsets.
5. Go back to the OPL offset corresponding to zero-OPD, and start to record data of interest: interferograms obtained by OPD scans (fringe exposure).
6. Integrate exposures for photometry in the same instrument configuration, first with beam A only; then with beam B only.

Usually the sensitivity is limited by the internal fringe tracking, which has to be performed with integration times that are shorter than the atmospheric coherence time.

#### 7.1.1 Target acquisition

When the operator starts an OB on the instrument the acquisition template begins. The sequence of this template starts by a “preset”: the target coordinates  $(\alpha, \delta)$  and the target proper motions are sent to the telescopes and the delay lines, so they can slew to the position corresponding to the target coordinate at preset time. Once the telescopes are tracking and Coudé-guiding, i.e. the adaptive optics loops are closed on both telescopes, the target can be seen in the FOV of MIDI in imaging mode. To ensure beam interference, the images from both beams must be overlapped. The beam overlap is performed by either:

- Using the IRIS guiding system (see 5.2). IRIS will offset the telescopes to bring the target photocenter onto the reference pixels (defined for the IRIS vs. MIDI alignment) of its detector. IRIS guarantees that the beam overlap is kept by sending corrections to the telescopes. **Experience has shown an acquisition accuracy of the order of 0.15 pixels with IRIS.** This method will be used as default.
- Using the MIDI acquisition image setup and its associated script that repeats several iterations of the sequence: star photocenter measurement, then offsets calculated and sent to the telescope to bring the star image on a reference pixel of the detector. The

loop stops when the error vector for both beams is smaller than a pre-defined threshold (0.7 pixel). This method is now considered as obsolete and is used only if the target is too faint for IRIS, or on specific user request in case the acquisition images are of scientific value.

The user has a possibility to use a guide star for the Coudé systems, different from the target. **For details and limits see the VLT user manual.**

### 7.1.2 Fringe search

Once beams are overlapped, fringes can be obtained provided VLTI delay line positions yield a zero-OPD ( $\pm 30 \mu\text{m}$ ). In this case, scanning the OPD with the MIDI piezo-mounted mirrors will yield interferograms.

In absence of an external fringe tracker, fringe search for MIDI consists in doing several scans at different delay line position offsets. These offsets are within a range around the expected zero-OPD value (given by an OPD model), and the incremental step of the offset is adjusted for covering the whole fringe search range given by piezo scans. The fringe search is normally executed in “fast” mode: 500- $\mu\text{m}$  OPD steps between two scans, and dispersion using the grism to get the maximum coherence length. For targets with low correlated flux fringes can be searched in “slow” mode. The search mode is decided by the instrument operator with view on the target parameters given by the user.

### 7.1.3 Fringe measurement in Fourier mode

Once the delay line offset that yields the zero-OPD is found, a batch of interferograms will be recorded in a series of scans to form an exposure. Group-delay measurements are used to correct the position of the tracking delay-line. If the “SCI\_PHOT” setup is used, chopping (synchronized with the scans) is performed in order to remove at data reduction time the thermal background from the photometric channels. This does not affect the fringe tracking.

### 7.1.4 Photometry

With the “HIGH\_SENS” setup and in order to compute the fringe visibility from interferograms, it is necessary to measure the flux from each beam through the beam combiner separately, using the same optical set up as for fringe measurement. Two exposures are therefore taken, with the MIDI shutter at different positions (beam-A open only, then beam-B open only).

Similar exposures are also taken in SCI\_PHOT, since they can be used to refine the photometry measured in the photometric channels during the fringe exposure. **For P89, the number of frames for the photometry can be adjusted by the user. See the MIDI template manual for details.**

## 7.2 Total sequence timing

As said in Sect.6.2 for MIDI in P89 the average time to get a calibrated visibility point is 50 minutes in service mode (SCI-CAL). Hence, the time to complete the above tasks is 25 minutes. This value includes all the overheads. The variable duration of the photometry exposures (set by the user) has a minor impact on the OB execution time.

Visitor mode is usually allocated for targets that require a non-standard acquisition procedure (i.e., very faint target, no Coudé guide star existing, target that is embedded in a complex structure in IR, etc..). In this case, 30 minutes of overheads for the scientific target observation are granted, and the allocated time to get a calibrated visibility is 80 minutes.

### 7.3 The VLT software environment for phase-2

Observations are described by Observing Blocks (OBs). A standard OB consists of:

- A target coordinate set.
- A target acquisition template.
- A set of observation templates for data collection.
- A constraint set.
- A list of intervals of the local sidereal times at which the observations shall be executed.

The templates are the atoms of an OB sequence. They represent the simplest units of an observation and are described extensively in the Template Manual. The P2PP software enables users to create lists of targets. For each target one or several OBs can be created with P2PP by selecting templates and by filling request keyword values (free parameters of the templates) and intervals of the local sidereal times at which the observations shall be executed. The P2PP user manual is available at the ESO website:

<http://www.eso.org/sci/observing/phase2/P2PP/P2PPDocumentation.html>

For a detailed description of the MIDI templates, please refer to the P89 “MIDI Template Manual”. This document will be available online with the announcement of observing time (web letters).

### 7.4 Post-observation process

#### 7.4.1 Data handling

Data from the MIDI instrument will be stored as FITS binary table files.

Because of the high frame rate of the MIDI detector, the amount of produced data is bulky. One should expect at least 1.2 Gbyte of raw data for each calibrated visibility measurement. To ease data handling, an exposure is split into several 100-Mbyte files (if the exposure is larger than this size), and a file containing the information about the organization of the exposure in multiple files is generated.

#### 7.4.2 The pipeline

Information concerning the pipeline (quick data processor to assess the validity of exposure data) and the data quality control can be found on the web at:

<http://www.eso.org/observing/dfq/quality/>

For the data reduction, there are several IDL packages: MIA (developed by MPIA), EWS (developed by Leiden Observatory), OYSTER (an interface for MIA and EWS). More information can be found at:



<http://www.mpia-hd.mpg.de/MIDISOFT/mia.html>

<http://www.eso.org/~chummel/midi/midi.html>

### **7.4.3 Data distribution**

For any information on the ESO data distribution policy, please check the webpage:

<http://www.eso.org/sci/observing/phase2/DataRelease.html>

---oOo---